Neutral-gas depletion and repletion in plasmas

A. Fruchtman[1,2] and J.-M. Rax[2]
[1]*H.I.T.-Holon Institute of Technology, 52 Golomb St., Holon 58102, Israel*
[2]*Laboratoire de Physique des Plasmas, École Polytechnique-Université de Paris XI, 91128 Palaiseau, France*

(Received 2 October 2009; accepted 25 February 2010; published online 6 April 2010)

Repletion of neutrals, an unexpected increase in the neutral-gas density when ionization is intense, has been recently predicted to occur in a gas discharge when a thermalized neutral gas is collisionless enough, so that its inertia dominates over the drag by collisions with ions. A parameter is identified here that determines which process should occur, neutral-gas repletion or the more expected neutral-gas depletion. The particle and momentum balance equations of the plasma and neutrals are solved, and it is demonstrated how when this parameter is varied, the neutral-gas density exhibits a transition between depletion and repletion. © *2010 American Institute of Physics*. [doi:10.1063/1.3368041]

I. INTRODUCTION

Space and laboratory plasmas can be significantly affected when ionization is so intense that the neutral-gas density is modified. The effect of neutral-gas density modification in gas discharges has already been addressed in early studies.[1–4] However, only in recent years, with the growing use of lower pressure and higher power radio-frequency discharges, is the importance of neutral-gas density modification becoming fully recognized.[5–34]

Usually, the modification of the neutral-gas density as a result of a strong ionization is a depletion of the neutrals; the neutral-gas density is expected to decrease when the ionization is intense. Such neutral-gas depletion has been indeed measured[5–22] and explained theoretically.[23–33] However, Raimbault *et al.*[26] showed that if collisions with ions of a thermalized neutral gas are rare enough, so that its inertia dominates over the drag by collisions with ions, the neutral-gas density increases rather than decreases when ionization is intense. We have shown that such an unexpected effect, coined by us a neutral-gas repletion, should occur in such a collisionless neutral gas whenever its equation of state is such that the neutral-gas pressure increases when the neutral-gas density increases.[28,30] We further showed that, indeed, neutral-gas repletion is not expected to occur when such collisionless neutrals move ballistically into the discharge without mutual collisions, since in this case their equation of state is such that the neutral-gas pressure is larger where the neutral-gas density is lower.[28,30]

In the present paper we assume that the neutrals are thermalized, their pressure is higher where their density is higher, and in particular we assume that they are isothermal. As said above, if such neutrals are collisionless, so that their pressure term is balanced by their inertia term in the momentum equation, they should experience repletion. If, instead, collisions with ions balance the neutral-gas pressure gradient, there should be a neutral-gas depletion. We therefore take into account in the momentum balance of the neutrals both the drag term due to collisions with ions and the inertia term. We show that, indeed, as the drag by the ions becomes smaller, intense ionization results in repletion of the neutrals. The drag by the ions is smaller at a lower gas pressure, what leads to a larger role of the gas inertia, which, in turn, results in the neutral-gas repletion.

In Sec. II we present the model for the plasma and for the neutral gas. The plasma is assumed to be collisionless as the drag by the neutrals is small relative to the ion inertia.

In the neutral-gas dynamics we take into account both drag due to collisions with ions and neutral inertia. In Sec. III we write the equations in a dimensionless form for a gas discharge between two plane boundaries. In Sec. IV we derive an expression for the neutral-gas density as a function of the plasma density and analyze the parameter space. In Sec. V and in Sec. VI we discuss, correspondingly, neutral-gas depletion and repletion. In Sec. VII we analyze the spatial profiles of plasma and neutral-gas densities. In Sec. VIII numerical examples are presented.

II. THE MODEL

We consider a one-dimensional quasineutral plasma, in which all variables depend on x only. The momentum equations for the plasma and for the neutrals are

$$\frac{\partial}{\partial x}(mnv^2 + nT) = -mk\Gamma(N+n) \tag{1}$$

and

$$\frac{\partial}{\partial x}(mNV^2 + NT_g) = mk\Gamma(N+n), \tag{2}$$

respectively. Here m is the ion (or neutral) mass, N and n are the neutral-gas and plasma densities, V and v are the neutral-gas and plasma velocities, T_g and T are the neutral and electron temperatures, and k is the ion-neutral collision rate constant. The ion temperature is assumed smaller than the electron temperature and is therefore neglected here. The electrons are assumed to have a Boltzmann distribution. The drag force is written in this form since there is no net mass flow so that the plasma particle flux density Γ is equal in size

(and opposite in direction) to the neutral-gas particle flux density,

$$\Gamma = nv = -NV. \tag{3}$$

The continuity equation is

$$\frac{\partial \Gamma}{\partial x} = \beta N n, \tag{4}$$

where β is the electron-neutral collisional ionization rate constant.

So far, the equations are symmetric with respect to the plasma and the neutrals. We now restrict ourselves to the common situation that the neutral-gas density is much larger than the plasma density. The drag force [the right-hand side (RHS) of Eqs. (1) and (2)] is then approximated as $mkN\Gamma$. Because of that assumption, the ion inertia term in the momentum equation is larger than the neutral inertia term,

$$\frac{m\Gamma^2}{n} \gg \frac{m\Gamma^2}{N}. \tag{5}$$

Previously, the case that both ions and neutrals are collisional,

$$mkN\Gamma \gg \frac{m\Gamma^2}{n} \gg \frac{m\Gamma^2}{N}, \tag{6}$$

as well as the case that both ions and neutrals are collisionless,

$$\frac{m\Gamma^2}{n} \gg \frac{m\Gamma^2}{N} \gg mkN\Gamma, \tag{7}$$

have been studied. In the collisional case neutrals are depleted,[23] while, in contrast, in the collisionless case a repletion has been predicted.[26] The repletion was shown to occur when neutrals are collisionless but thermalized, so that their pressure increases as their density increases.[28,30] We continue here to adopt the assumption that the neutrals are thermalized and their pressure increases as the density increases. In particular, we assume that the neutrals are isothermal, and that their pressure is NT_g, T_g being the neutral-gas temperature. However, we extend the analysis to the regime

$$\frac{m\Gamma^2}{n} \gg \frac{m\Gamma^2}{N} \approx mkN\Gamma. \tag{8}$$

The plasma ions are still assumed to be weakly collisional, the drag term due to ion-neutral collisions is assumed to be much smaller than the ion inertia term. However, no assumption is made about the relative sizes of the drag term due to ion-neutral collisions and the neutral inertia term. Therefore both neutral-gas depletion and neutral-gas repletion may occur, and we study the transition between these depletion and repletion.

Since the drag term is still assumed to be smaller than the ion inertia term, as said above, the plasma ions are still approximated as weakly collisional. We neglect the RHS of Eq. (1), and the plasma momentum balance is approximated as

$$\frac{m\Gamma^2}{n} + nT = n_0 T. \tag{9}$$

Here, n_0 is the maximal plasma density and $v=0$ where the plasma density is maximal. The drag term due to ion-neutral collisions is kept in the neutral-gas momentum equation, so that the neutral-gas momentum balance is

$$\frac{\partial}{\partial x}\left(\frac{m\Gamma^2}{N} + NT_g\right) = mkN\Gamma. \tag{10}$$

The governing equations are therefore Eqs. (9), (10), and (4) for n, N, and Γ.

III. THE CONFIGURATION

Let us assume that a plasma is formed between two walls a distance $2a$ apart. The plasma is symmetric with respect to the middle plane located at $x=0$. We also assume that the electron temperature T is uniform. We solve for the plasma and neutral-gas variables for $0 \le x \le a$. The governing equations, in dimensionless coordinates, are

$$\frac{\bar{\Gamma}^2}{4\bar{n}} + \bar{n} = 1, \tag{11}$$

$$\frac{\partial}{\partial \xi}\left(r\frac{\bar{\Gamma}^2}{\bar{N}} + \bar{N}\right) = s\bar{N}\bar{\Gamma}, \tag{12}$$

and

$$\frac{\partial \bar{\Gamma}}{\partial \xi} = \frac{ps}{r}\bar{N}\bar{n} = \frac{2\beta N_W a}{c}\bar{N}\bar{n}, \tag{13}$$

where the dimensionless variables and coordinate are

$$\bar{n} \equiv \frac{n}{n_0}, \quad \bar{N} \equiv \frac{N}{N_W}, \quad \bar{\Gamma} \equiv \frac{2\Gamma}{n_0 c}, \quad \xi \equiv \frac{x}{a}, \tag{14}$$

while the dimensionless parameters are

$$p \equiv \frac{\beta n_0}{kN_W}, \quad r \equiv \frac{n_0^2 c^2}{4N_W^2 c_N^2}, \quad s \equiv \frac{n_0 cka}{2c_N^2}. \tag{15}$$

Here $c \equiv \sqrt{T/m}$ and $c_N \equiv \sqrt{T_g/m}$ are the plasma and neutral-gas acoustic velocities. Note that $\bar{n}$ varies between 1 and 0.5, $\bar{N}$ equals unity at the boundary (N_W is the neutral-gas density at the boundary), and $\bar{\Gamma}$ varies between zero and unity. The numerical factor 4 appears in the plasma equation and does not appear in the neutral-gas equation because of the different values of $\bar{n}(=0.5)$ and $\bar{N}(=1)$ at $\xi=1$.

We also note that according to Eq. (11), the plasma Mach number is related to the normalized plasma density as

$$M \equiv \frac{v}{c} = \sqrt{\frac{1-\bar{n}}{\bar{n}}}. \tag{16}$$

The Mach number at the plasma boundary equals unity.

IV. DEPENDENCE OF NEUTRAL-GAS DENSITY ON PLASMA DENSITY

Employing Eqs. (12) and (13), we write

$$\frac{\partial}{\partial \bar{\Gamma}}\left(r\frac{\bar{\Gamma}^2}{\bar{N}}+\bar{N}\right)=\frac{r\bar{\Gamma}}{p\bar{n}}. \tag{17}$$

Using $\bar{\Gamma}^2=4\bar{n}(1-\bar{n})$ from Eq. (11), we integrate Eq. (17) to

$$4r\frac{\bar{n}(1-\bar{n})}{\bar{N}}+\bar{N}-\bar{N}(0)=\frac{4r}{p}(\ln\sqrt{\bar{n}}+1-\bar{n}). \tag{18}$$

The neutral-gas density at the center of the discharge turns out to be

$$\bar{N}(0)=1+r\left(1-\frac{p_c}{p}\right), \tag{19}$$

where

$$p_c \equiv 2(1-\ln 2)=0.613\ 71. \tag{20}$$

It is clear from this form that

$$\text{if } p<p_c, \quad \text{then } \bar{N}(0)<1, \tag{21}$$

which corresponds to neutral-gas depletion, while

$$\text{if } p>p_c, \quad \text{then } \bar{N}(0)>1, \tag{22}$$

which corresponds to a neutral-gas repletion. The parameter p determines whether neutral-gas depletion or neutral-gas repletion be the dominant process. When p is smaller or larger than the critical value p_c, neutral-gas depletion or repletion occurs.

With Eqs. (18) and (19), we can rewrite the equation for the neutral-gas density as

$$4r\frac{\bar{n}(1-\bar{n})}{\bar{N}}+\bar{N}-1-r=\frac{2r}{p}(\ln 2\bar{n}+1-2\bar{n}). \tag{23}$$

We may now write an explicit expression for $\bar{N}(\bar{n})$,

$$\bar{N}=\frac{1+r+(2r/p)(\ln 2\bar{n}+1-2\bar{n})+\sqrt{[1+r+(2r/p)(\ln 2\bar{n}+1-2\bar{n})]^2-16r\bar{n}(1-\bar{n})}}{2}. \tag{24}$$

For certain values of p and r, $\bar{N}(\bar{n})$ is real and positive for all values of $\bar{n}\in[0.5,1]$. Then, $\bar{N}(\bar{n})$ either varies monotonically or nonmonotonically as a function of $\bar{n}$. Since $\bar{n}$ always decreases from the center of the discharge toward the boundary, the variation in $\bar{N}$ with $\bar{n}$ also reflects its variation with ξ. It is convenient to analyze the behavior of $\bar{N}(\bar{n})$ by introducing two new parameters,

$$q\equiv\frac{1+r}{2\sqrt{r}}, \quad b\equiv\frac{\sqrt{r}}{p}, \tag{25}$$

so that $\sqrt{r}=q-\sqrt{q^2-1}$ and $p=(q-\sqrt{q^2-1})/b$. Despite the increase in the number of parameters, the analysis is made easier when the new parameters are used. With these two new parameters, Eq. (24) is rewritten as

$$\bar{N}=(q-\sqrt{q^2-1})\{q+b(\ln 2\bar{n}+1-2\bar{n}) +\sqrt{[q+b(\ln 2\bar{n}+1-2\bar{n})]^2-2\bar{n}(2-2\bar{n})}\}. \tag{26}$$

Equivalent to Eq. (19), we write the neutral-gas density at the center of the discharge as

$$\bar{N}(0)=2(q-\sqrt{q^2-1})[q-b(1-\ln 2)]. \tag{27}$$

The value of $\bar{N}$ is real when the discriminant of the polynomial in $\bar{N}$ in Eq. (23) is positive for all values of $\bar{n}\in[0.5,1]$. It is straightforward to show that the domain in the (b,q) plane, where this happens, is

$$q\geq q_{\min}(b), \tag{28}$$

where

$$\text{if } b\leq 1 \text{ then } q_{\min}=1 \quad \text{and}$$
$$\text{if } b\geq 1 \text{ then } q_{\min}=b\left[1-\ln\left(\frac{2b^2}{1+b^2}\right)\right]. \tag{29}$$

A surprising result of the analysis here is the possible existence of nonmonotonic density profiles of the neutral gas. This nonmonotonicity results from the neutral-gas dynamics being dominated by different terms, either inertia, pressure gradient, or drag due to collisions, in different regions. Formally, the profile of the neutral-gas density is nonmonotonic when $d\bar{N}/d\bar{n}=0$ for some value of $\bar{n}\in[0.5,1]$. Such nonmonotonic profiles occur for

$$q_d(b)\geq q\geq q_r(b), \tag{30}$$

where

$$q_d=\frac{1+b^2}{b}-b\ln 2, \tag{31}$$

and

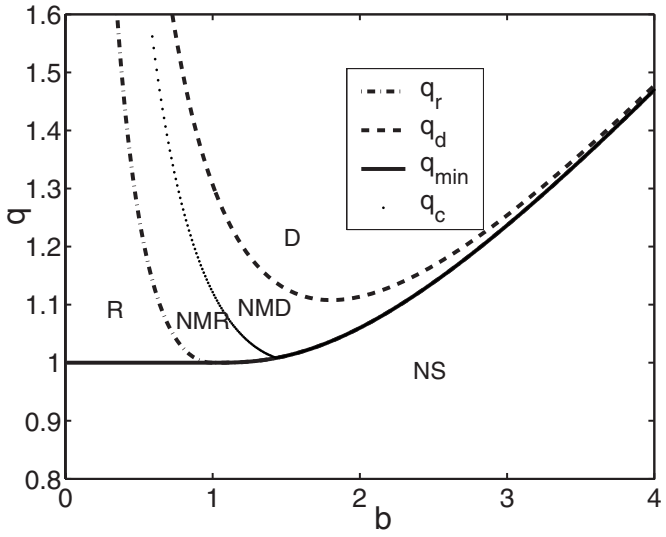

FIG. 1. The various domains in the (b,q) plane. The domains of depletion $[\bar{N}(0)<1]$ are denoted as D ($\bar{N}$ is monotonically decreasing toward the center of the discharge) and NMD (when it is nonmonotonic). The domains of repletion $[\bar{N}(0)>1]$ are denoted as R ($\bar{N}$ is monotonically increasing toward the center of the discharge) and NMR (when it is nonmonotonic). See the text for the expressions for the dividing lines q_r, q_d, $q_{\min}$, and q_c.

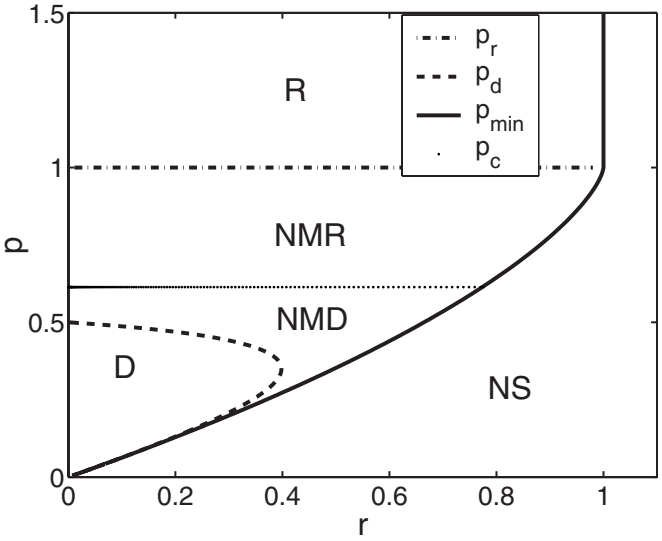

FIG. 2. The various domains in the (r,p) plane equivalent to those in Fig. 1 in the (b,q) plane. The domains of depletion $[\bar{N}(0)<1]$ are denoted as D ($\bar{N}$ is monotonically decreasing toward the center of the discharge) and NMD (when it is nonmonotonic). The domains of repletion $[\bar{N}(0)>1]$ are denoted as R ($\bar{N}$ is monotonically increasing toward the center of the discharge) and NMR (when it is nonmonotonic). The dividing lines p_r, p_d, $p_{\min}$, and p_c are equivalent to those in Fig. 1.

$$\text{if } b \le 1 \text{ then } q_r = \frac{1+b^2}{2b}, \quad \text{and}$$
$$\text{if } b \ge 1 \text{ then } q_r = q_{\min}. \tag{32}$$

According to Eqs. (21) and (22), the curve that divides the (b,q) plane into domains of depletion and repletion is

$$q = q_c = \frac{1+p_c^2 b^2}{2p_c b}. \tag{33}$$

Figure 1 presents the division of the (b,q) plane into the various domains, following the analysis above. The domain where $\bar{N}$ is not real is denoted as NS. The domains of depletion $[\bar{N}(0)<1]$ are denoted as D (when the neutral-gas density is monotonically decreasing toward the center of the discharge) and NMD (when it is nonmonotonic). The domains of repletion $[\bar{N}(0)>1]$ are denoted as R (when the neutral-gas density is monotonically increasing toward the center of the discharge) and NMR (when it is nonmonotonic). Figure 2 presents the equivalent division of the (r,p) plane into the various domains with the same notations as in Fig. 1. Figure 3 shows seven examples of profiles of $\bar{N}$ as functions of $\bar{n}$. The examples have been chosen to demonstrate the various different profiles and they belong to the four different domains shown both in Figs. 1 and 2. Four of the examples are for neutral-gas depletion and three for repletion.

In Secs. V and VI, we analyze further the depletion and repletion.

V. NEUTRAL-GAS DEPLETION

Of the four profiles of neutral-gas density in Fig. 3 that exhibit depletion, the first three profiles correspond to points in the domain D in Figs. 1 and 2. The fourth profile corresponds to a point in the domain NMD, the profile is nonmonotonic. Specifying different values for $\bar{N}(0)$, we determine different curves in the (r,p) plane that satisfy Eq. (19). Four such curves are shown in Fig. 4, a figure which other-

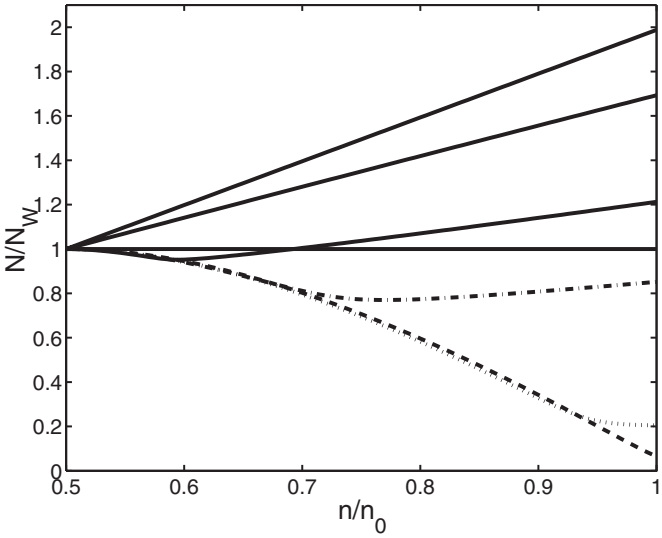

FIG. 3. Normalized neutral-gas density as a function of the normalized plasma density for the cases: (1) $p=0.001$, $r=10^{-7}$, $s=1.1416$ (solid horizontal line), (2) $p=0.01$, $r=0.0155$, $s=6.1952$ (dashed line), (3) $p=0.1$, $r=0.1548$, $s=3.7144$ (dotted line), (4) $p=0.5$, $r=0.6518$, $s=1.3841$ (dashed-dotted line), (5) $p=0.8$, $r=0.9125$, $s=1.0181$, (6) $p=2$, $r=1$, $s=0.7600$, and (7) $p=50$, $r=1$, $s=0.6698$. The three last lines are solid, showing an increased neutral repletion as p increases.

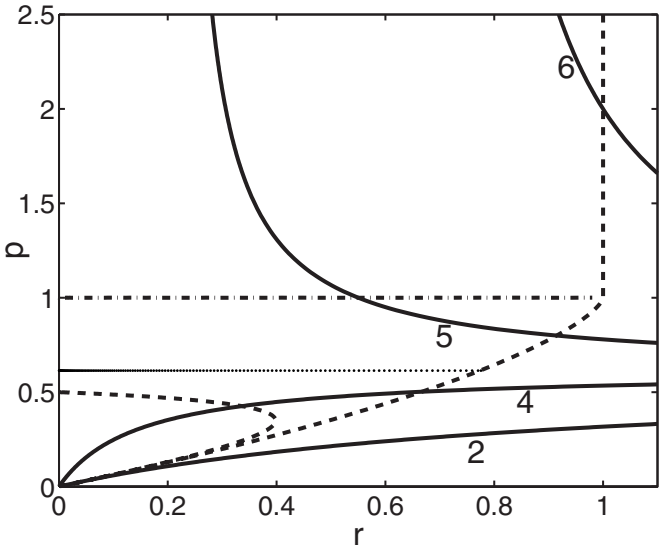

FIG. 4. Four solid lines satisfying Eq. (19) with constant $\bar{N}(0)$: 0.0643 (curve 2), 0.8518 (curve 4), 1.2125 (curve 5), and 1.5268 (curve 6). Curves 2 and 4 exhibit depletion while curves 5 and 6 exhibit repletion. The pairs of (r,p) of cases 2, 4, 5, and 6 in Fig. 3 fall on the curves denoted here by the same numbers. The domains are the same as in Fig. 2. The parts of the curves in NS do not represent physical profiles of $\bar{N}(0)$.

wise shows the same domains in the (r,p) plane as Fig. 2 does. Curves 2 and 4 are so denoted in Fig. 4 because the pairs of values of r and p of the second example and of the fourth example in Fig. 3 correspond to points in the (r,p) plane that fall on these curves. Curve 4, for which there is a small depletion, $\bar{N}(0)=0.8518$, passes through both domains D and NMD. Curve 2, for which there is a large depletion, $\bar{N}(0)=0.0643$, is mostly in the unphysical domain NS (in which $\bar{N}$ is not always real). The part of the curve that corresponds to real values of $\bar{N}$ is near the origin of the plane, namely, for small values of r and p.

We can approximately find the upper bounds on p and on r for which there are such physical solutions. The analysis turns out to be easier when one employs b and q. For a given $\bar{N}(0)$, which is much smaller than unity, b and q are much larger than unity. Equation (27) is then approximated to $q\cong(1-\ln 2)b/[1-\bar{N}(0)]$. Physical solutions exist for $q\geq q_{\min}$, where $q_{\min}$ is defined in Eq. (29). The inequality is satisfied for $q\geq\sqrt{(1-\ln 2)/\bar{N}(0)}$. From the relation $\sqrt{r}\cong 1/(2q)$ for a large q, we find the upper bounds on r and on p for a large depletion,

$$\text{if } \bar{N}(0)\ll 1, \text{ then } r\leq\frac{\bar{N}(0)}{2p_c} \quad \text{and} \quad p\leq\frac{\bar{N}(0)}{2}. \tag{34}$$

The values of r and p at the point of entrance of curve 2 into the domain NS in Fig. 4 indeed are given by Eq. (34) with the equality signs. Note that there are no solutions with a full depletion, $\bar{N}(0)=0$. According to Eq. (19), for a large neutral depletion $\bar{N}(0)\ll 1$, in addition to the conditions in Eq. (34), the parameters r and p should be near the line

$$r=\frac{p}{p_c}. \tag{35}$$

According to Eqs. (34) and (35), large neutral-gas depletion occurs when $rp_c\cong p\ll 1$. Employing the explicit expressions for r and p [Eq. (15)], we express the conditions for a large depletion as

$$p=\frac{\beta n_0}{kN_W}\ll 1, \quad r=\frac{n_0^2c^2}{4N_W^2c_N^2}\cong\frac{\beta n_0}{kN_W 2(1-\ln 2)} \tag{36}$$

or

$$\frac{(1-\ln 2)n_0c^2}{2N_Wc_N^2}\cong\frac{\beta}{k}\ll\frac{N_W}{n_0}. \tag{37}$$

Depletion follows ion-neutral collisions being dominant. We turn now to the case of a large repletion.

VI. NEUTRAL-GAS REPLETION

Three profiles of the neutral-gas density shown in Fig. 3 exhibit repletion. The profile number 5 is nonmonotonic, corresponding to a point in the domain NMR, while the other two profiles are monotonic, corresponding to points in the domain R. Similar to the depletion case, curves 5 and 6 are so denoted in Fig. 4 because the pairs of values of r and p of the fifth profile and of the sixth profile in Fig. 3 correspond to points in the (r,p) plane that fall on these curves. Curve 5, for which there is a small repletion, $\bar{N}(0)=1.2125$, passes through both domains R and NMR. Curve 6, for which there is a larger repletion, $\bar{N}(0)=1.5268$, lies in the R domain.

Since $r\leq 1$, large repletion only occurs when $p\gg 1$. The profile of the neutral-gas density when the repletion is high, $r=1$ and $p\gg 1$, is

$$\bar{N}_r=1+\sqrt{1-4\bar{n}(1-\bar{n})}. \tag{38}$$

The maximal neutral-gas density, at the center of the discharge, is twice the neutral-gas density at the wall, $\bar{N}_r$ $(\bar{n}=1)=2$. We note that in this case in which $r=1$ the neutral-gas acoustic velocity is $c_N=n_0c/(2N_W)$ and the neutral-gas velocity is written as

$$|V|=\frac{\Gamma}{N}=\frac{n_0c}{2N_W}\frac{2\sqrt{\bar{n}(1-\bar{n})}}{[1+\sqrt{1-4\bar{n}(1-\bar{n})}]}$$
$$=c_N\frac{2\sqrt{\bar{n}(1-\bar{n})}}{[1+\sqrt{1-4\bar{n}(1-\bar{n})}]}\leq c_N. \tag{39}$$

The neutral-gas velocity at the wall equals in this case of large repletion the neutral-gas acoustic velocity, $V(\bar{n}=0.5)=c_N$.

Large neutral-gas repletion occurs therefore when

$$\frac{\beta n_0}{kN_W}\gg 1, \quad r=\frac{n_0^2c^2}{4N_W^2c_N^2}\cong 1 \tag{40}$$

or

$$\frac{n_0 c^2}{4N_W c_N^2} \cong \frac{N_W}{n_0} \ll \frac{\beta}{k}. \tag{41}$$

Repletion follows ion-neutral collisions being abundant. Until here we analyzed how the neutral-gas density varies across the discharge as a function of the plasma density. In the rest of the paper we analyze the spatial dependencies of the neutral-gas and plasma densities. We also discuss the relation between the input and output parameters of the discharge.

VII. THE DENSITY PROFILES

Using Eqs. (11) and (13) we write ξ as a function of $\bar{n}$,

$$\int_{\bar{n}}^{1} \frac{(2\bar{n}'-1)d\bar{n}'}{\sqrt{\bar{n}'(1-\bar{n}')}\bar{n}'\bar{N}(p,r,\bar{n}')} = \frac{ps}{r}\xi, \tag{42}$$

where $\bar{N}(p,r,\bar{n})$ is given by Eq. (24). Integrating up to the plasma boundary, we obtain a solvability condition,

$$\int_{0.5}^{1} \frac{(2\bar{n}-1)d\bar{n}}{\sqrt{\bar{n}(1-\bar{n})}\bar{n}\bar{N}(p,r,\bar{n})} = \frac{ps}{r}. \tag{43}$$

This equation determines a relation between the three characteristic parameters, p, r, and s. The solvability condition for a specified neutral-gas density usually determines the electron temperature T as an eigenvalue.[35–40]

We first briefly comment on the well-known case of a uniform neutral-gas density, $\bar{N} \cong 1$. Equations (42) and (43) are then easily integrated. We split each integral into two parts for the two terms in the numerator. For the first integral we change the independent variable into $\sqrt{\bar{n}'}$, while for the second integral we integrate with respect to $1/\sqrt{\bar{n}'}$. The resulting density profile, in an implicit form, and the solvability condition become

$$4 \arccos\sqrt{\bar{n}} - 2\sqrt{\frac{1}{\bar{n}}-1} = \frac{ps}{r}\xi, \quad \pi - 2 = \frac{ps}{r} = \frac{2\beta N_W a}{c}. \tag{44}$$

As said above, this is viewed as an equation for the eigenvalue T. In this case of a specified uniform neutral-gas density, T is specified independently of the plasma density n_0. We also note that these relations can be equivalently written for the plasma Mach velocity:[39] $\arctan(M) - M = (ps/2r)\xi = (\beta N_W a/c)\xi$.

In the general case, when $\bar{N}$ is modified by the discharge, the solvability condition determines the value of one unknown parameter. This would usually be the temperature T if n_0 is viewed as known. Sometimes, a power balance equation is also considered and provides an additional relation between T and n_0.

In Sec. VIII, we turn to numerical solutions of the full equations.

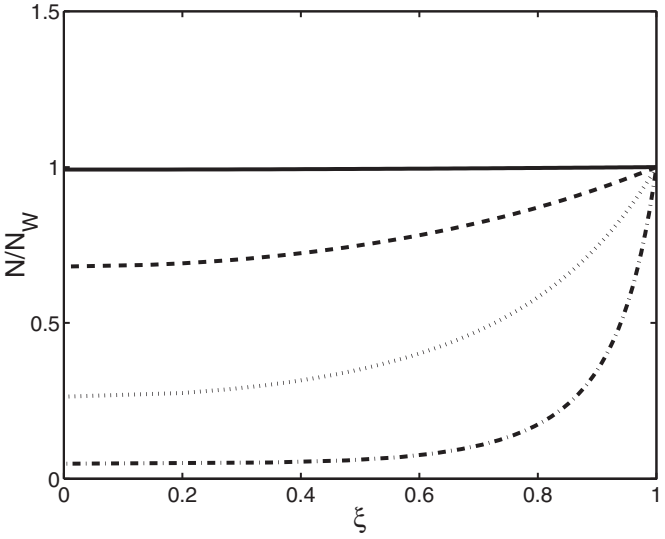

FIG. 5. The normalized neutral-gas density profiles when $N_W = 2 \times 10^{20}$ m^{-3} for $n_0/N_W = 0.0001$, $T = 2.182$ eV ($p = 3.1 \times 10^{-6}$, $r = 4 \times 10^{-8}$) by a solid line, $n_0/N_W = 0.005$, $T = 2.259$ eV ($p = 2 \times 10^{-4}$, $r = 10^{-4}$) by a dashed line, $n_0/N_W = 0.02$, $T = 2.471$ eV ($p = 0.0015$, $r = 0.0018$) by a dotted line, and $n_0/N_W = 0.075$, $T = 3.012\,35$ eV ($p = 0.0196$, $r = 0.0314$) by a dashed-dotted line. In Figs. 5–10, $T_g = 0.135$ eV, $a = 0.05$ m, and the gas is argon.

VIII. NUMERICAL EXAMPLES

We present here numerical solutions for Eqs. (42) and (43). We usually solve the equations for the discharge steady state when the geometry, the values of the neutral-gas variables at the boundary, and the power are specified. Instead of specifying the power, we specify here n_0 and determine T as an eigenvalue through solving Eq. (43). Then the values of the dimensionless parameters p, r, and s are determined.

Figures 5–10 show the density profiles of the neutrals $\bar{N}(\xi)$ and plasma $\bar{n}(\xi)$. Here the geometry is specified by specifying $a = 0.05$ m, the gas is argon, and in all the examples the neutral-gas temperature is taken as T_g

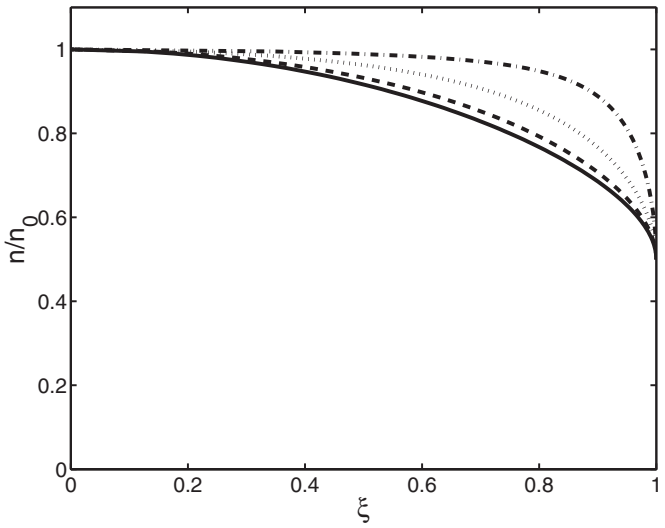

FIG. 6. The normalized plasma density for the same four cases as in Fig. 5, denoted accordingly by lines of the same style.

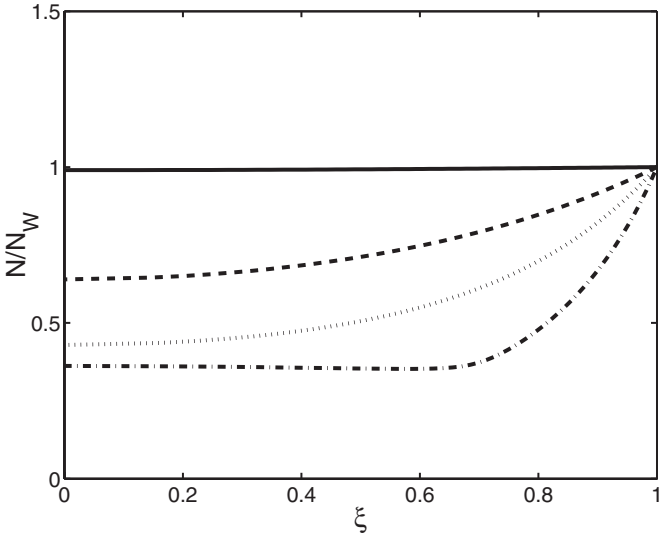

FIG. 7. The normalized neutral-gas density profiles when $N_W=2\times10^{19}$ m^{-3} for $n_0/N_W=0.001$, $T=3.216$ eV ($p=3.7\times10^{-6}$, $r=6\times10^{-8}$) by a solid line, $n_0/N_W=0.05$, $T=3.421$ eV ($p=0.0258$, $r=0.0158$) by a dashed line, $n_0/N_W=0.11$, $T=3.635$ eV ($p=0.0766$, $r=0.0815$) by a dotted line, and $n_0/N_W=0.20$, $T=3.8901$ eV ($p=0.0196$, $r=0.2882$) by a dashed-dotted line. In Figs. 5–10, $T_g=0.135$ eV, $a=0.05$ m, and the gas is argon.

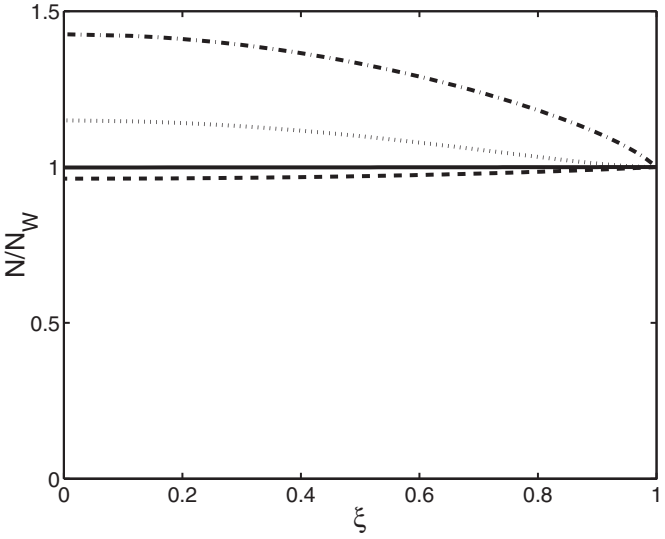

FIG. 9. The normalized neutral-gas density profiles when $N_W=2\times10^{18}$ m^{-3} for $n_0/N_W=0.001$, $T=6.12$ eV ($p=0.0052$, $r=1.1\times10^{-5}$) by a solid line, $n_0/N_W=0.05$, $T=6.18$ eV ($p=0.2658$, $r=0.0286$) by a dashed line, $n_0/N_W=0.2$, $T=5.92$ eV ($p=0.9315$, $r=0.4385$) by a dotted line, and $n_0/N_W=0.3$, $T=5.553$ eV ($p=1.137$, $r=0.9255$) by a dashed-dotted line. In Figs. 5–10, $T_g=0.135$ eV, $a=0.05$ m, and the gas is argon.

$=0.135$ eV. For the calculation, the ion-neutral collision rate constant (p. 63 in Ref. 38) has been taken as

$$k = 8.99\times10^{-10}\left(\frac{\alpha_R}{A_R}\right)^{1/2}\ \text{cm}^3/\text{s}, \tag{45}$$

where A_R (=20 for argon) is the reduced mass in atomic mass units and a_R (=11.1 for argon) is the relative polarizability. For a Maxwellian electron distribution, we choose the approximated expression for the ionization rate constant as

$$\beta = \sigma_0 v_{te}\exp\left(-\frac{\epsilon_i}{T}\right), \tag{46}$$

where $v_{te}\equiv(8T/\pi m_e)^{1/2}$ is the electron thermal velocity and $\sigma_0\equiv\pi(e^2/4\pi\epsilon_0\epsilon_i)^2$, ϵ_0 being the permittivity of the vacuum and ϵ_i (=15.6 eV for argon) the ionization energy.

For each pair of figures, Figs. 5 and 6, Figs. 7 and 8, and Figs. 9 and 10, we specified a different value of the neutral-gas density at the boundary N_W. Such is $N_W=2\times10^{20}$ m^{-3} in Figs. 5 and 6, $N_W=2\times10^{19}$ m^{-3} in Figs. 7 and 8, and $N_W=2\times10^{18}$ m^{-3} in Figs. 9 and 10. For each pair of figures, Figs. 5 and 6, Figs. 7 and 8, and Figs. 9 and 10, for which the value of N_W is specified, several values of n_0 (or n_0/N_W) are specified. As said above, specifying n_0 is instead of specifying the deposited power. For each such value of n_0/N_W, the value of T is calculated through the solution of Eq. (43), as mentioned above. For such specified n_0/N_W and T, the values of the parameters p, r, and s are determined (and given in the figure captions). Once p and r are specified, the density profile is found through

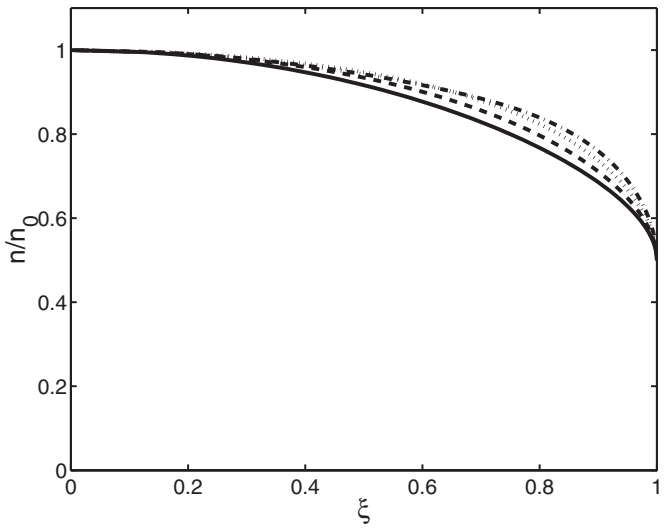

FIG. 8. The normalized plasma density for the same four cases as in Fig. 7, denoted accordingly by lines of the same style.

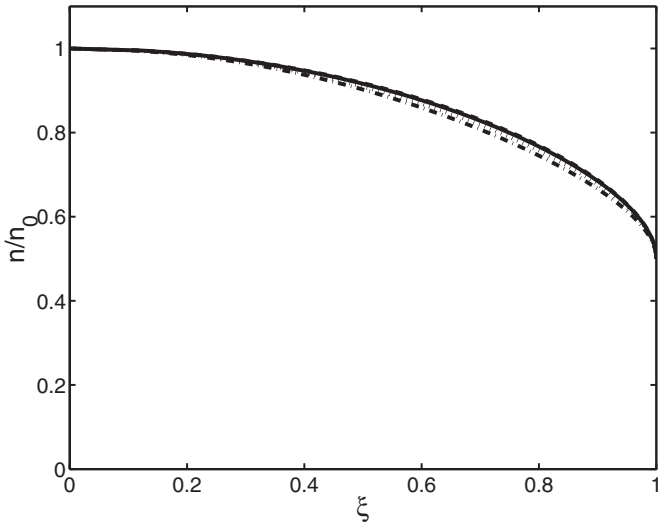

FIG. 10. The normalized plasma density for the same four cases as in Fig. 9, denoted accordingly by lines of the same style.

$$\int_{\bar{n}}^{1} \frac{(2\bar{n}'-1)d\bar{n}'}{\sqrt{\bar{n}'(1-\bar{n}')}\bar{n}'\bar{N}(p,r,\bar{n}')} \Bigg/ \int_{0.5}^{1} \frac{(2\bar{n}-1)d\bar{n}}{\sqrt{\bar{n}(1-\bar{n})}\bar{n}\bar{N}(p,r,\bar{n})} = \xi, \tag{47}$$

which is obtained by dividing Eq. (42) by Eq. (43) and by use of Eq. (24) for $\bar{N}(p,r,\bar{n})$.

The three pairs of figures show the transition from neutral-gas depletion to repletion as the value of N_W is reduced. In Figs. 5 and 6, in which N_W is relatively large, neutral-gas depletion is dominant and increases as n_0/N_W is increased. The drag on the neutrals due to collisions with ions dominates over the neutral inertia. This is reflected in the small value of the parameter p. When r and p approximately satisfy Eq. (35), neutral-gas depletion is almost complete. In Fig. 6, the density profile of the plasma is flatter for a higher plasma density, a signature of neutral-gas depletion.[23]

In Figs. 7 and 8, the specified neutral-gas density at the boundary is smaller than in Figs. 5 and 6. Neutral-gas depletion, shown in Fig. 7, is smaller, as neutral-gas inertia plays a larger role. One neutral-gas density profile is nonmonotonic. The parameters r and p in this case belong to the domain NMD in Figs. 1 and 2. As seen in Fig. 7, the neutral-gas density has a local maximum at the center of the discharge, although its value is lower than at the boundary. This is due to the larger role of neutral inertia than in the first case, shown in Figs. 5 and 6. Also, due to the smaller neutral-gas depletion in this case, the plasma density shown in Fig. 8 is less flat than in Fig. 6.

The third case is shown in Figs. 9 and 10. The specified neutral-gas density at the boundary is lower than in the two previous examples. As plasma density is increased, there is first a neutral-gas depletion (shown by a dashed line). As the plasma density is increased further, neutral-gas repletion becomes dominant, as is shown by two lines for two larger values of plasma density. For the dotted line there is already repletion, since $p=0.9315>2(1-\ln 2)=0.613\,71$ [Eq. (22)]. The dashed-dotted line shows a case for which p is larger than unity. Neutral repletion is dominant in these two last curves but does not reach its maximal possible value, described by Eq. (38). Neutral inertia dominates in this case over the neutral-gas drag by collisions with ions. The plasma density in Fig. 10 is slightly more peaked in this case of neutral-gas repletion, opposite to the flatter plasma profile in the case of neutral-gas depletion.

IX. SUMMARY

We showed here that neutrals under strong ionization can exhibit very different behaviors. If they are thermalized and isothermal, as in the examples in the present paper, their density can either increase or decrease as a result of strong ionization, depending on the relative strengths of the inertia term and the drag term in their momentum equation. When the drag due to collisions with ions is dominant, the more expected neutral-gas depletion occurs as a result of intense ionization. If, however, the neutral-gas inertia is dominant over the drag by collisions with ions, the less expected neutral-gas repletion should occur. A dimensionless parameter has been identified that if it is larger or smaller than a certain critical value, neutral-gas depletion or repletion is expected to occur. Numerical examples have been presented that show that, as neutral-gas density at the discharge boundary is reduced, a transition occurs from neutral-gas depletion to neutral-gas repletion.

In contrast to neutral-gas depletion, which has been recently observed in several gas-discharge experiments, neutral-gas repletion has not been observed so far. For the occurrence of neutral-gas repletion, neutrals should simultaneously be thermalized while the drag by collisions with ions should be negligible. These conditions are not easily satisfied. However, such conditions, either in laboratory or space, that will induce neutral-gas repletion, might evolve. The analysis here unfolded what the conditions for neutral-gas repletion to occur are.

ACKNOWLEDGMENTS

A.F. gratefully acknowledges the support of École Polytechnique during his research visit to LPP. This research was partially supported by the Israel Science Foundation (Grant No. 864/07).

[1] J. E. Allen and P. C. Thonemann, Proc. Phys. Soc. London, Sect. B **67**, 768 (1954).
[2] A. Caruso and A. Cavaliere, Br. J. Appl. Phys. **15**, 1021 (1964).
[3] P. C. Stangeby and J. E. Allen, J. Phys. A: Gen. Phys. **4**, 108 (1971); J. Phys. D **6**, 224 (1973).
[4] H. B. Valentini, J. Phys. D **17**, 931 (1984).
[5] R. W. Boswell and K. Porteous, Appl. Phys. Lett. **50**, 1130 (1987).
[6] I. D. Sudit and F. F. Chen, Plasma Sources Sci. Technol. **5**, 43 (1996).
[7] J. Gilland, R. Breun, and N. Hershkowitz, Plasma Sources Sci. Technol. **7**, 416 (1998).
[8] A. W. Degeling, T. E. Sheridan, and R. W. Boswell, Phys. Plasmas **6**, 1641 (1999); **6**, 3664 (1999).
[9] S. Yun, K. Taylor, and G. R. Tynan, Phys. Plasmas **7**, 3448 (2000).
[10] E. J. Tonnis and D. B. Graves, J. Vac. Sci. Technol. A **20**, 1787 (2002).
[11] H. Abada, P. Chabert, J. P. Booth, J. Robiche, and G. Gartry, J. Appl. Phys. **92**, 4223 (2002).
[12] C. Watts and J. Hanna, Phys. Plasmas **11**, 1358 (2004).
[13] B. Clarenbach, M. Krämer, and B. Lorenz, J. Phys. D **40**, 5117 (2007).
[14] J. E. Maggs, T. A. Carter, and R. J. Taylor, Phys. Plasmas **14**, 052507 (2007).
[15] M. Shimada, G. R. Tynan, and R. Cattolica, Plasma Sources Sci. Technol. **16**, 193 (2007).
[16] A. M. Keesee and E. E. Scime, Rev. Sci. Instrum. **77**, 10F304 (2006); Plasma Sources Sci. Technol. **16**, 742 (2007).
[17] A. Aanesland, L. Liard, G. Leray, J. Jolly, and P. Chabert, Appl. Phys. Lett. **91**, 121502 (2007).
[18] D. O'Connell, D. L. Crintea, T. Gans, and U. Czarnetzki, Plasma Sources Sci. Technol. **16**, 543 (2007).
[19] D. O'Connell, T. Gans, D. L. Crintea, U. Czarnetzki, and N. Sadeghi, J. Phys. D **41**, 035208 (2008).

[20]D. O'Connell, T. Gans, D. L. Crintea, U. Czarnetzki, and N. Sadeghi, Plasma Sources Sci. Technol. **17**, 024022 (2008).
[21]D. L. Crintea, U. Czarnetzki, S. Iordanova, I. Koleva, and D. Luggenholscher, J. Phys. D: Appl. Phys. **42**, 045208 (2009).
[22]C. M. Denning, M. Wiebold, and J. E. Scharer, Phys. Plasmas **15**, 072115 (2008).
[23]A. Fruchtman, G. Makrinich, P. Chabert, and J. M. Rax, Phys. Rev. Lett. **95**, 115002 (2005).
[24]A. Fruchtman, "The effect of the magnetic field profile on the plume and on the plasma flow in the Hall thruster," in *Proceedings of the 29th International Electric Propulsion Conference* (Electric Rocket Propulsion Society, Cleveland, OH, 2005), IEPC Paper No. 2005-068.
[25]A. Fruchtman, "Neutral depletion and pressure balance in plasma," in 33rd European Physical Society Conference on Plasma Physics, Rome, Italy, edited by F. De Marco and G. Vlad (2006), Vol. 30I, Paper No. D-5.013.
[26]J.-L. Raimbault, L. Liard, J.-M. Rax, P. Chabert, A. Fruchtman, and G. Makrinich, Phys. Plasmas **14**, 013503 (2007).
[27]L. Liard, J.-L. Raimbault, J.-M. Rax, and P. Chabert, J. Phys. D **40**, 5192 (2007).
[28]A. Fruchtman, IEEE Trans. Plasma Sci. **36**, 403 (2008).
[29]A. Fruchtman, Plasma Sources Sci. Technol. **17**, 024016 (2008).
[30]A. Fruchtman, G. Makrinich, J.-L. Raimbault, L. Liard, J.-M. Rax, and P. Chabert, Phys. Plasmas **15**, 057102 (2008).
[31]J.-L. Raimbault and P. Chabert, Plasma Sources Sci. Technol. **18**, 014017 (2009).
[32]A. Fruchtman, Plasma Sources Sci. Technol. **18**, 025033 (2009).
[33]L. Liard, J.-L. Raimbault, and P. Chabert, Phys. Plasmas **16**, 053507 (2009).
[34]A. Fruchtman, Phys. Plasmas **17**, 023502 (2010).
[35]W. Schottky, Phys. Z. **25**, 635 (1924).
[36]J. R. Forrest and R. N. Franklin, Br. J. Appl. Phys. **17**, 1569 (1966); R. N. Franklin, *Plasma Phenomena in Gas Discharges* (Clarendon, Oxford, 1976).
[37]V. A. Godyak, *Soviet Radio Frequency Discharge Research* (Delphic Associates, Falls Church, VA, 1986).
[38]M. A. Lieberman and A. J. Lichtenberg, *Principles of Plasma Discharges and Materials Processing* (Wiley, New York, 1994).
[39]A. Fruchtman, G. Makrinich, and J. Ashkenazy, Plasma Sources Sci. Technol. **14**, 152 (2005).
[40]N. Sternberg, V. Godyak, and D. Hoffman, Phys. Plasmas **13**, 063511 (2006).